Modeling of a Spray-Drying Process for the Encapsulation of High-Added Value Extracts from Food by-Products

Andrea Bassani[a*], Daniele Carullo[a], Francesco Rossi[b], Cecilia Fiorentini[a], Guillermo D. Garrido[a], Gintaras V. R. Reklaitis[b], Irene Bonadies[c], Giorgia Spigno[a]

[a]Università Cattolica del Sacro Cuore, Department for Sustainable Food Process (DiSTAS), Via Emilia Parmense 84, 29122 Piacenza, Italy

[b]Purdue University, Forney Hall of Chemical Engineering, 480 Stadium Mall Drive, West Lafayette, IN 47907, United States

[c]Italian National Research Council CNR, Institute for Polymers, Composites and Biomaterials (IPCB-CNR), Via Campi Flegrei 34, Comprensorio "A. Olivetti", 80078 Pozzuoli (NA), Italy

*Corresponding author: Eng. Andrea Bassani
E-mail address: andrea.bassani@unicatt.it (A. Bassani)
Tel: (+39) 0523 599178
Fax: (+39) 0523 599232

Abstract

The main goal of this research was to develop a mathematical model for a co-current spray drying-assisted encapsulation of natural extracts from grape pomace and citrus fruit peels, aiming to predict both structural features and the retention of their bioactive constituents. Model validation was performed using a laboratory scale spray dryer, analyzing the product in terms of moisture content, solids and total phenolic compounds recovery yields. The comparison between experimental and simulated results revealed that the model properly described the system. A slight effect of air inlet temperature was observed on the phenolic content of produced particles. For this reason, a novel kinetic law, which allows predicting the degradation of phenols was proposed and validated. These results highlighted the potential of spray-drying technology to efficiently encapsulate high-added value compounds with good preservation of their bioactive compounds, offering the possibility to decrease food waste issues while improving industry economical benefits.

Keywords: spray-drying, mathematical modeling, natural extracts, antioxidants, bioeconomy.

1. Introduction

Residues of agri-food industries, being considered as "one among the most generated bio-wastes around the globe" (Dahiya et al., 2018), have long been the subject of studies to minimize and prevent the negative impact on either economics or environment associated with their disposal (Kaderides & Goula, 2019; Pataro et al., 2017; Sepelevs et al., 2020). Currently, the majority of this biomass does not find full exploitation, since it is utilized as a low added value animal feed/fertilizer or directly burned to produce bioenergy (Aliakbarian et al., 2015; Galanakis et al., 2012, 2015).

On the other hand, agri-food wastes offer the possibility to create new opportunities and markets since these substrates are of particular interest for food, pharmaceutical, and cosmetic industries especially due to their capability to retain large amounts of "natural" high-added-value reusable materials (Chandrasekaran, 2013). In particular, wastes deriving from fruit and vegetable industrial processing, which account for about 50% by weight all around the world (Galanakis, 2015), represent a rich source of highly antioxidant species like polyphenols, generally recovered by means of a solid-liquid extraction step (Frontuto et al., 2019; Oliveira et al., 2018; Zanoni et al., 2020; Waterhouse et al., 2017). Such compounds are a heterogeneous group of secondary plant metabolites having different molecular structures, among which non-flavonoid phenolic acids, non-flavonoid stilbenes, anthocyanins, flavonols, flavanols, tannins, flavones, and flavanones (Spigno et al., 2014).

Polyphenols are characterized by remarkable health-promoting properties with strong immunomodulatory, antimicrobial, and anti-inflammatory actions (Aliakbarian et al., 2015; Archaina et al., 2017; Zhang et al., 2020), which enable their potential integration in the formulation of food products as radical scavengers or as protective agents against cancer or cardiovascular diseases (Chasekioglou et al., 2017; Goula & Lazarides, 2015; Frontuto et al., 2019).

Nevertheless, these bioactive compounds are easily prone to degradation phenomena, being sensitive to multiple environmental factors such as temperature, pH, moisture, light, and oxygen, which greatly limit their range of application at the industrial scale (Toledo-Madrid et al., 2019; Zhang et al., 2020).

Therefore, in order to improve the stability of phenolic compounds and, hence, preserve their health benefits when utilized as food ingredients, an encapsulation step is strictly required (Kaderides & Goula, 2019; Utpott et al., 2020).

In particular, spray-drying technology has been widely applied for microencapsulation purposes due to its easy scalability, flexibility, low processing costs, and capability to produce low water-content particles, thus enhancing their microbiological stability with increased shelf life, as well as ensuring a controlled release of entrapped bioactives (Ding et al., 2020; Gharsallaoui et al., 2007; Toledo-Madrid et al., 2019). Within this frame, several previous authors have reported the successful encapsulation of phenolic compounds extracted from food wastes as assisted by the spray-drying technique (Aliakbarian et al., 2015; Jurmanovic et al., 2019; Osorio-Arias et al., 2020; Permal et al., 2020a, b; Sormoli & Langrish, 2016; Waterhouse et al., 2017; Zanoni et al., 2020). Moreover, spray-drying encapsulation could be also applied to increase the thermal stability of natural extracts to be included in bioplastic film before extrusion (Bassani et al., 2019).

The microencapsulation process via spray-drying is essentially based on three consecutive operations, carried out onto a fluid feed where either bioactives or coating material are dispersed, namely the preparation, homogenization, and atomization in the drying chamber. In particular, the latter step is necessary to increase the water transfer from the feed to the drying medium (e.g. pressurized hot air) and to produce spherical particles with the desired distribution of sizes. However, the control of end product features, including either morphological (e.g. shape, size, density, porosity) or quantitative (e.g. recovery yield of mass/bioactives, extent of degradation, encapsulation efficiency, humidity) aspects, could be achieved by employing predictive models optimizing the main processing parameters, among which the inlet/outlet drying gas temperature and the nature/concentration of coating material in the feed formulation (Cotabarren et al., 2018; Lisboa et al., 2018; Schmitz-Schug et al., 2016). Additionally, the synergy between both considered parameters is of utmost importance to ensure stability/integrity of encapsulated compounds, with no or negligible loss of their functionality (Georgetti et al., 2008; Langrish, 2009).

79 To the best of our knowledge, despite several authors have previously adopted mathematical tools
80 (e.g. computational fluid dynamics (CFD), multiple regression analysis, response surface
81 methodology (RSM)) to predict the behavior of samples during a spray-drying process (Cotabarren
82 et al., 2018; Sormoli & Langrish, 2017; Wang & Langrish, 2009; Zbicinski, 2017), only few works
83 were devoted to study the degradation kinetics of antioxidant compounds, such as lycopene or vitamin
84 C, as affected by the operating variables (Goula & Adamopoulos, 2005, 2006; Langrish, 2009).
85 For the reasons explained above, the main objective of this work was to develop and validate a
86 suitable model of co-current spray-drying for natural extract encapsulation with particular reference
87 to grape skins and citrus fruit peels, being selected based on their high content in antioxidant
88 polyphenols (Bassani et al., 2019; Spigno et al., 2007).
89 Firstly, experimental data were collected using a laboratory-scale spray-drier by testing the effect of
90 different combinations of drying gas inlet temperature and molar ratio of coating material/natural
91 extract on the properties of obtained powder. Subsequently, a mathematical model including mass,
92 energy, and momentum balances, as well as a correlation for the distribution of particle size and
93 phenolics degradation kinetics, was implemented and applied to simulate the previous runs. Finally,
94 the model simulation and the experimental results were compared.

95

96 ## 2. Materials and Methods

97 ### *2.1. Raw materials and chemicals*

98 In this work, two different natural extracts were used and obtained, respectively, from grape skins of
99 "*Barbera*" variety, which were gently provided by a winery located in the Piedmont region, and from
100 citrus fruit peels, purchased in a ready-to-use powdered form by the "Evesa S.A." company (Cadìz,
101 Spain). For this reason, only grape skins were subjected to a solid-liquid extraction (SLE) step in
102 order to provide an extract to be furtherly used for spray-drying tests. To this purpose, the SLE step
103 was carried out by mixing the grape skins with aqueous ethanol (60%, v/v) at a solid-to-liquid ratio

of 1:8 (g/mL), and the obtained mixture was then stirred at 3500 rpm (mixer Silverson, L5M, producer) for 1 h at 60 °C (Amendola et al., 2010). Afterward, the solids were separated from the liquid by centrifugation (Thermo Scientific SL 16 R) at 2000 g for 15 minutes at room temperature, and the latter was concentrated twice under vacuum at 40 °C with a B-114 rotary evaporator (BÜCHI Labortechnik AG, Flawil, Switzerland) and stored under refrigerated conditions until its use.

Gallic acid and sodium carbonate were purchased from Fluka (Milan, Italy); ethanol and Folin-Ciocalteau reagent were supplied by VWR Chemicals (Milan, Italy), while maltodextrins (Glucidex IT 12 DE (dextrose equivalent)) and β-cyclodextrins (KLEPTOSE) were obtained from Roquette Italia s.p.a. (Alessandria, Italy).

2.2. Spray-drying process

Experimental trials for the encapsulation of natural extracts were executed employing a laboratory-scale spray dryer (Büchi Mini Spray Dryer B-290, Switzerland), equipped with an atomization cylinder (0.48 m in height, 0.16 m in diameter). The liquid feed was sent to the drying system via a peristaltic pump (model, producer) working at a constant flow rate of 4 mL/min. Compressed air at 38.5 m^3/h was used to co-currently disperse the liquid in fine droplets through a 0.7 mm nozzle to be subsequently dried in the atomization cylinder. For each test, the aspiration rate was set at 100%, with the obtained powder being collected into a cyclone separator and stored for further analyses.

One disadvantage of this laboratory spray dryer is related to the angle of exit of the particles from the nozzle (assumed to be equal to 55°). Indeed, during the process, some particles end up against the wall of the atomization cylinder, thus leading to a reduction of the global mass yield of the process, defined according to Eq. (1):

$$Recovery\ yield\ (\%) = \frac{m_P}{m_{th,feed}} \quad (1)$$

where m_P is the mass of recovered powder on dry matter (in g) and $m_{th,\,feed}$ is the theoretical amount of solids present in the feed (in g).

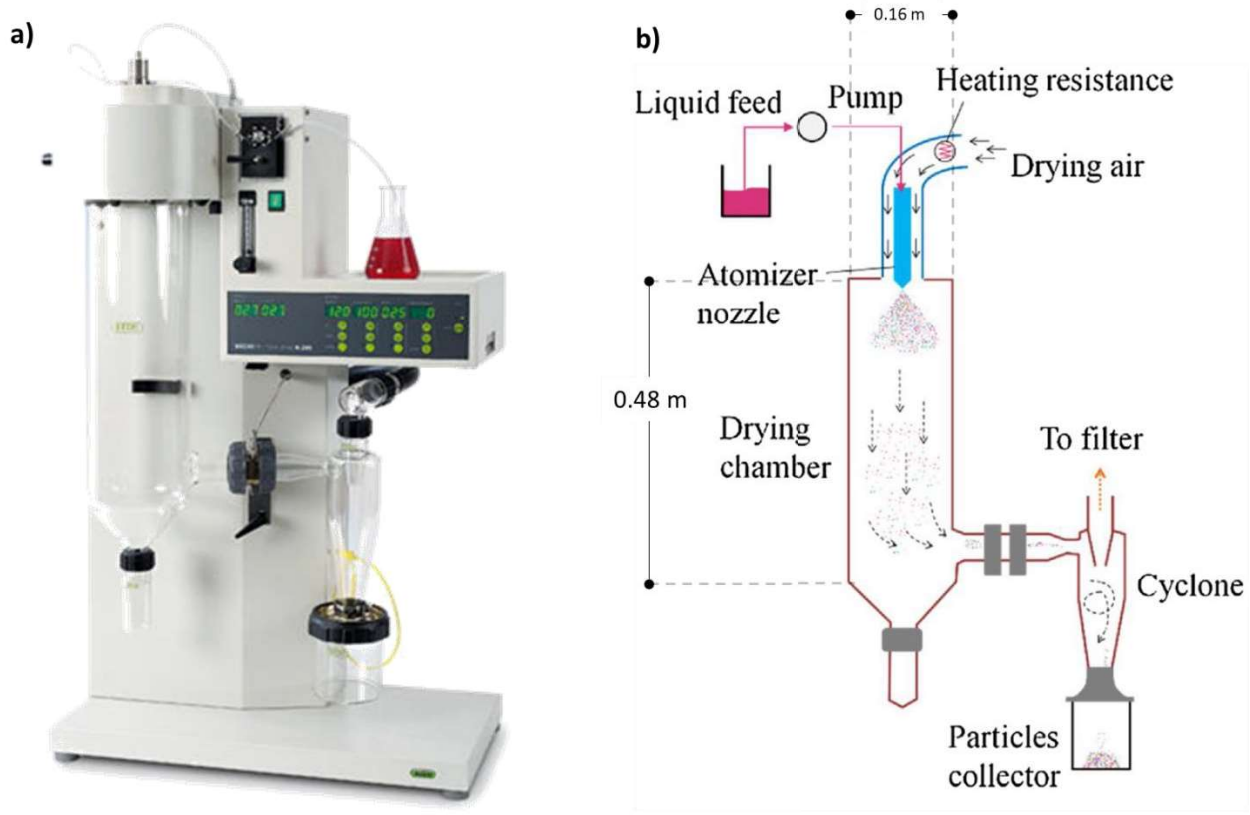

Figure 1. Büchi Mini Spray Dryer B-290 (a) and schematic representation of the spray dryer (Cotabarren et al., 2018) with the related dimensions of interest (b)

During the experimental campaign, maltodextrin (MD) was used as a carrier for extracts from grape skins.

As for the case of grape skins extracts, a first set of experiments was performed at variable drying air inlet temperature (T = 120, 150, and 180°C) and at constant molar ratio (dextrose equivalent/ gallic acid equivalent = DE/GAE) of 2.5 mol_{DE}/mol_{GAE}. Instead, only at 120°C and at 150°C, experiments were also carried out by varying the molar ratio within the range 0.3 – 2.54 mol_{DE}/mol_{GAE}, obtained by mixing the extracts with different amounts of maltodextrins.

In addition, in the framework of the European project Newpack, drying tests on citrus fruit peel extracts, with cyclodextrin (CD) as carrier, were carried out at constant processing conditions, which

were set at 120°C of air inlet temperature and at a constant cyclodextrins/extract ratio of 0.75 (w/w). Briefly one of the aims of Newpack project was to evaluate the potential incorporation of encapsulated (with CD) citrus natural extracts into PLA/PHB films. Cyclodextrin was selected for both a higher physical and/or chemical stability (Marques, 2010) and a lower antimicrobial activity if compared to maltodextrin (Velazquez-Martinez et al., 2021). Indeed, cyclodextrin could not support microbial growth, while maltodextrins could, with the risk of reducing the antimicrobial activity of the extract. Therefore, the data of CD-citrus extract were used just to further validate the model developed starting from grape skin extracts.

2.3. Spray-drying modeling

In this section, the model equations and the assumptions made are shown. In particular, only the main parameters and equations are presented, with the latter being properly modified, while the clear and in-deep description of the whole set of equations is given by Sormoli and Langrish (2016) and Truong et al. (2005). The equations have been implemented in Microsoft Visual Studio C++ 2019 and the numerical routines for the solution of the ordinary differential equations (ODE) system have been taken in the BzzMath library (Buzzi-Ferraris and Manenti, 2015).

2.3.1. Momentum balance

The droplet velocity is described by Eqs. (2) and (3), which take into account both the axial (v_{px}) and radial (v_{pr}) trajectory, respectively. Moreover, due to the mechanical characteristic of the spray dryer, the tangential component of the velocity vector was neglected.

$$\frac{dv_{px}}{dh} = \frac{\left(1 - \frac{\rho_a}{\rho_p}\right) g - \frac{\frac{3}{4}\,\rho_a C_d v_r\,(v_{px} - v_{ax})}{\rho_p d_p}}{v_{px}} \tag{2}$$

$$\frac{dv_{pr}}{dh} = -\frac{\frac{3}{4}\,\rho_a C_d v_r\,(v_{px} - v_{ax})}{\rho_p d_p\, v_{px}} \tag{3}$$

where h is the axial distance from the atomizer (in m), ρ_a and ρ_p are the densities of air and particle, respectively (in kg/m^3), g is the gravity acceleration (in m/s^2), C_d is the drag coefficient (-), v_r is the relative velocity between the droplet and the air (in m/s), v_{ax} is the component of air velocity along the x-direction, and d_p is the droplet diameter (in m).

2.3.2. Mass balance

The unsteady-state mass balances for both the single droplet and the total water removed during drying are reported in Eqs. (4) and (5), respectively:

$$\frac{dm_p}{dh} = -\frac{\xi A_p\, K_p (p_{vs} - p_{vb})}{v_{px}} \tag{4}$$

$$\frac{dY_b}{dh} = \sum_{droplets} \frac{\left(-\frac{dm_p}{dh}\right) n_{droplets}}{G} \tag{5}$$

where m_p is the mass of the particle or droplet (in kg), ξ is the relative drying rate, evaluated as reported by Truong et al (2005), A_p is the droplet surface area (in m^2), K_p is the mass transfer coefficient (in kg/(m ·s ·Pa)), p_{vs} is the partial pressure of water vapor at the droplet surface (in Pa), p_{vb} is the partial pressure of water vapor in the bulk air (in Pa), Y_b is the bulk gas humidity on dry basis (in kg$_{vapor}$/kg $_{dry\ air}$), G is the mass flow rate of the dry air (in kg/s), and $n_{droplets}$ is the flow rate of droplets (in s^{-1}).

2.3.3. Heat balance

The unsteady-state heat balances for the single droplet and the bulk air are reported in Eqs. (6) and (7), respectively:

$$\frac{dT_p}{dh} = \frac{A_p\, H\left(T_g - T_p\right) + \left(-\frac{dm_p}{dh}\right)\left(\Delta H_{vap.} + q_{stn}\right)}{m_p\, C_{p,mix}\, v_{px}} \quad (6)$$

$$\frac{dH_g}{dh} = \frac{1}{G}\left(\sum_{droplets} m_p C_{p,mix}\, \frac{dT_p}{dh} n_{droplets} - \frac{UA\left(T_g - T_{out}\right)}{H_{spray}}\right) \quad (7)$$

where T_p and T_g are the particle and gas temperatures (in K), respectively, H is the heat transfer coefficient for convection (in W/(m^2 · K)), evaluated using the equations reported by Troung et al. (2005), $\Delta H_{vap.}$ is the latent heat of water vaporization (in J/kg) (Green & Perry, 2008), q_{stn} is the average net isosteric heat of sorption, considered equal to 70500.0 J/kg as reported by Sormoli and Langrish (2016), $C_{p,\,mix}$ is the specific heat capacity of the droplet (≈ 4187 J/(kg · K)), being a mixture of water, natural extract, and carrier agent, T_{out} is the ambient temperature (≈ 20°C), H_{spray} is the height of the spray drier (in m), and UA is the overall heat transfer coefficient multiplied by the surface area of the spray dryer (in W/K), evaluated by following the procedure provided by Hanus and Langrish (2007).

2.3.4. Sorption isotherms

In order to estimate the relative drying rate (ξ), an evaluation of the equilibrium moisture content of the solid must be performed. In particular, such a parameter is a function of the relative humidity of the gas, the temperature of the gas, and the nature of the solid and the liquid. The variation of the equilibrium moisture content with relative humidity at a constant temperature is called sorption isotherm. To this purpose, the equation proposed by Sormoli and Langrish (2016) was utilized (Eq. 8):

$$X_{eq} = \frac{X_m ck\psi}{(1 - k\psi)(1 - k\psi + ck\psi)} \quad (8)$$

where X_{eq} is the equilibrium moisture content on a dry basis (in $kg_{vapor}/kg_{\ dry\ solids}$), Ψ is the relative humidity of the gas, X_m is an empirical constant equal to 0.087, while c and k are empirical variables that were evaluated as a function of temperature according to Eqs. (9) and (10):

$$c = c_0 \exp\left(\frac{\Delta H_1}{RT}\right) \tag{9}$$

$$k = k_0 \exp\left(\frac{\Delta H_2}{RT}\right) \tag{10}$$

where c_0 and k_0 are equal to 0.4 and 0.8, respectively, while ΔH_1 and ΔH_2 are equal to 8258.0 and 730.0 respectively (in J/mol).

2.3.5. Kinetic law for the degradation of polyphenols

As already mentioned, one of the main aims of this study was to investigate and evaluate the reduction in phenolic content of natural extracts that can occur after the encapsulation through the spray dryer, both at the experimental and modeling level. For this purpose, a first-order kinetic law for polyphenols degradation was included in the model (Eq. 11):

$$r_{phe} = A_0 \exp\left(\frac{E_{ap}}{RT_p}\right) C_{phe} \tag{11}$$

where r_{PHE} is the phenolics degradation rate (in mg_{GAE}/s), A_0 is the pre-exponential Arrhenius factor (in kg/s), E_{ap} is the activation energy of the reaction (J/mol), C_{phe} is the concentration of the polyphenols (in mg_{GAE}/kg_{dm}). This leads to the following differential equation, that allows to evaluate the polyphenols degradation at different distance from the atomizer (Eq. 12):

$$\frac{dC_{phe}^{out}}{dh} = \frac{\left(F_{dry}C_{phe}^{in} - F_{dry}C_{phe}^{out} - r_{phe}\right)}{v_{px}m_{dry}} \tag{12}$$

222 Where F_{dry} is the dry flow rate of the particle (in kg/s), m_{dry} is the total treaded dry mass (in kg), while
223 *in* and *out* superscripts stand for inlet and outlet. It is important to underline that, given the innovative
224 nature of this kinetic law (Eq. 11), the involved parameters (i.e., A_0 and E_{ap}) have to be evaluated
225 using experimental data through non-linear regression numerical routines of Bzz-Math Library
226 (Buzzi-Ferraris and Manenti, 2010).

227

228 *2.3.6. Estimation of particle size distribution*

229 In this study, the size of the droplets is assumed to follow a log-normal distribution. Thus, in order to
230 define the mean value to be included into log-normal distribution, the equation reported by Green and
231 Perry (2008) was chosen for predicting the median of the droplet size distribution (d_{50}) for sprays
232 from two-fluid nozzles (Eq. 13):

233 $$d_{50} = K_t \, \rho_a{}^{-0.325} \left(\frac{\dot{m}_L}{\dot{m}_L U_L + \dot{m}_a U_a}\right)^{0.55} \quad (13)$$

234 where K_t is an empirical value equal to 0.008, $\dot{m}_L$ and $\dot{m}_a$ are the liquid feed rate and the atomization
235 gas rate (in kg/s), respectively, while U_L and U_a are the liquid velocity and the atomization gas
236 velocity (in m/s) respectively. Knowing d_{50}, it is possible to evaluate the mean value of log-normal
237 distribution.

238

239 *2.4. Analyses*

240 *2.4.1. Total phenolic compounds*

241 All the extracts and powders obtained from spray-drying tests were subjected to TPC measurements
242 adopting the Folin-Ciocalteau method, as previously reported by Amendola et al. (2010). For the
243 analysis, 25 mL of water, 0.5 mL of extract or diluted powder sample, 2.5 mL of undiluted Folin-

Ciocalteau reagent, and 5 mL of sodium carbonate (20%, v/v in water) were mixed, brought to 50 mL, and allowed to stand for 30 min at 40°C. A mixture of water and reagents was used as a blank. The absorbance of the reacting mixture was then spectrophotometrically measured at 750 nm.

Gallic acid, previously dissolved in aqueous ethanol, was used to generate a five-point standard calibration curve in a concentration range of 0.1-1.0 mg/L, and the results were expressed as mg of gallic acid equivalent (GAE) per L of extract (mg_{GAE}/L) or per g of dry weight powder (mg_{GAE}/g_{DWP}). However, in order to estimate the effect of drying temperature and carrier/extract molar ratio on the amount of obtained phenolic compounds from the spray-drying process, a recovery yield was calculated as follows (Eq. 14):

$$TPC\ recovery\ (\%) = \frac{TPC_{msr}}{TPC_{th.}} \quad (14)$$

where TPC_{msr} represents the amount of phenolic compounds detected in the collected powder by spectrophotometrical measurements, while $TPC_{th.}$ stands for the theoretical amount of polyphenols present in the collected powder. The latter parameter was calculated by considering the volume of extract subjected to spray-drying (in mL), the concentration of phenolics in the extract (in mg_{GAE}/L), and the mass recovery yield previously defined through the Eq. (1).

2.4.2. Moisture content (MC)

Approximately 5 g of the powder collected from the spray-drying process of extracts from grape skins or citrus fruit peels were placed into a pre-weighed ceramic crucible and dried in an oven (model, producer) at 105°C until constant mass was achieved. MC was gravimetrically determined by weighing the samples before and after drying on an analytical balance. The moisture content, expressed as g of water/100g of powder (%), was calculated as follows (Eq. 15):

$$MC\ (\%) = \frac{m_{P,t=0} - m_{DP}}{m_{P,t=0}} \quad (15)$$

where $m_{P,\,t=0}$ is the mass of powder before drying (in g), while m_{DP} is the mass of powder immediately after drying (in g).

2.5. Statistical analysis

All experiments and analyses were executed in triplicate, with the obtained results all reported as mean ± standard deviation (SD). ANOVA test was carried out in order to evaluate the influence of specific process variables on measured parameters. In case of significant influence, assessed at a 99 % confidence level, variance homogeneity was checked and Tukey's post-hoc test was applied for means discrimination ($p \leq 0.01$), together with the calculation of the F-value. The statistical analysis was performed using the IBM SPSS Statistics 19 software (SPSS Inc, Chicago, USA).

3. Results and Discussion

3.1. Modeling of spray-drying process for Barbera extracts

Barbera extract was initially analyzed in order to characterize the inlet feed, so as to properly evaluate the ratio DE/GAE previously defined. In particular, the dry matter has been measured in a stove at 105 ± 2 °C to constant weight and was equal to 72.45 ± 0.25 g/L, while extract density value, measured with Gibertini densimeter at 20°C, was 0.98 ± 0.09 g/mL. The total polyphenol content, evaluated with Folin-Ciocalteau assay, was equal to 14.61 ± 0.65 mg_{GAE}/L.

Once the extracts were characterized, the first step was to validate the proposed model based on the experimental data collected and reported in Table 1. A validation, with a similar procedure, was already reported in our previous work (Bassani et al., 2020). However, the model was improved with

288 particular reference to the sorption isotherm (see paragraph 2.3.4), and the related assessment of
289 equilibrium moisture content of the encapsulated particles. Before running the simulation, a statistical
290 analysis of the experimental data obtained was carried out in order both to verify the consistency of
291 the data collected and to make some preliminary considerations.

Table 1. Experimental (exp.) and simulated (sim.) powder recoveries, outlet air temperature, and powder moisture content as a function of the different working inlet temperatures and DE/GAE molar ratios. Values were reported as means ± standard deviations. For each set of experiments, different superscript lowercase letters within the same column indicate significant differences among samples ($p < 0.01$).

T_{air_in} (°C)	DE/GAE	Recovery (%)			T_{air_out} (ºC)			Moisture (%)		
		exp.	F-value	*sim.*	*exp.*	F-value	*sim.*	*exp.*	F-value	*sim.*
120	2.53	80.34 ± 2.58^{a}		81.50	66.0 ± 1.0^{a}		67.49	3.48 ± 0.13^{a}		2.17
150	2.53	81.64 ± 0.46^{a}	0.75	81.50	83.0 ± 2.0^{b}	361.50	80.81	3.65 ± 0.23^{b}	1.98	1.29
180	2.53	80.5 ± 0.50^{a}		81.50	97.0 ± 1.0^{c}		93.12	3.78 ± 0.19^{b}		0.80
120	1.12	86.24 ± 0.68^{a}		81.50	66.0 ± 0.0^{a}		66.66	5.43 ± 0.32^{a}		2.43
120	0.56	89.40 ± 1.35^{a}	0.98	81.50	66.0 ± 0.0^{a}	-	66.45	5.96 ± 0.26^{a}	59.74	2.50
120	0.28	83.91 ± 8.22^{a}		81.50	66.0 ± 0.0^{a}		66.33	7.58 ± 0.12^{b}		2.54
150	1.12	80.71 ± 8.19^{a}		81.50	83.0 ± 0.0^{a}		80.40	4.17 ± 0.23^{a}		1.37
150	0.56	83.86 ± 5.57^{a}	0.36	81.50	83.0 ± 0.0^{a}	-	80.12	5.35 ± 0.14^{b}	228.39	1.42
150	0.28	77.66 ± 11.76^{a}		81.50	83.0 ± 0.0^{a}		79.94	7.66 ± 0.23^{c}		1.46

Results show that, regardless of the considered air inlet temperature (120 – 180 °C) and feed composition (0.28 – 2.53 DE/GAE), no statistical differences could be detected among process recovery yield values ($p > 0.01$). On the other hand, the outlet moisture contents seem to be statistically different among them ($p < 0.01$) both with respect to different temperatures and initial composition.

Then, a first simulation of the model was carried and the results obtained are reported in Table 1. It is worth underlining that the coefficient related to the heat transfer (*UA*) was estimated to 6.485 W/K by following the procedure reported by Hanus and Langrish (2007). A good agreement between experimental and simulated data can be highlighted, as also reported by scatter diagrams of Figure 1, especially regarding the outlet air temperature. However, it is interesting to point out that the recovery yield is not influenced by temperature or components ratio (Figure 1a). At the same time, there are some discrepancies between experimental and simulated values in the case of outlet moisture content (Figure 1c).

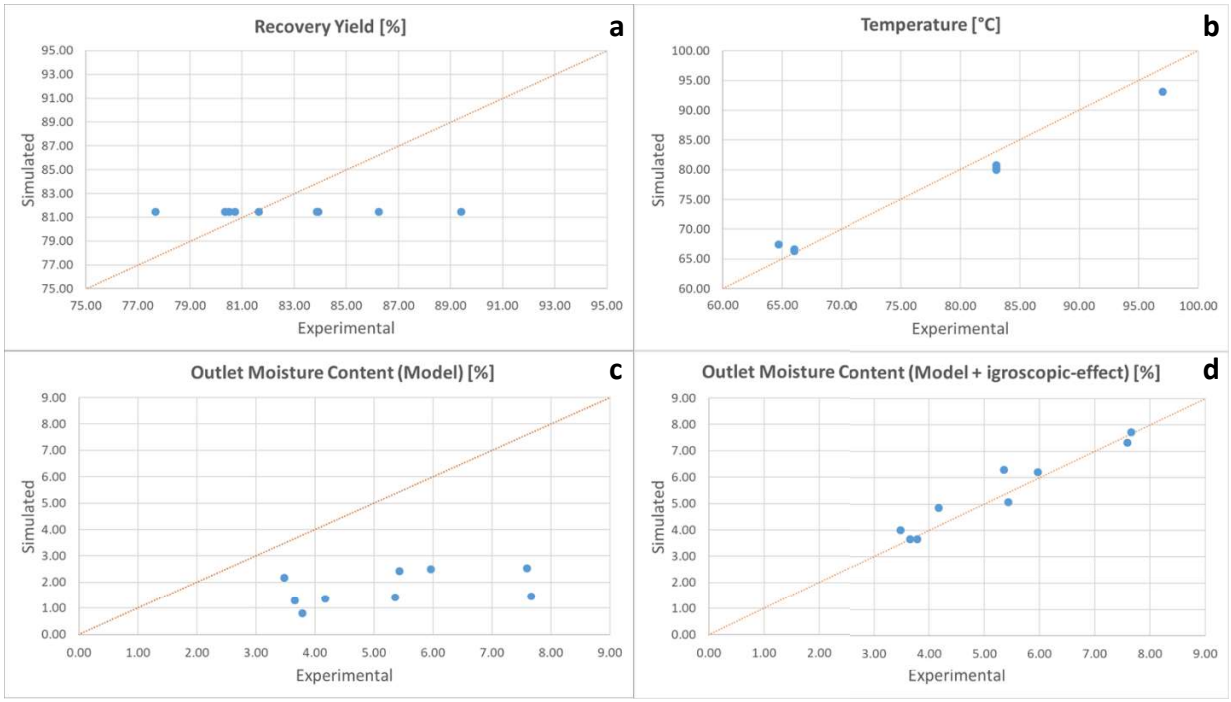

Figure 2. Scatter diagrams of recovery yields (a), outlet air temperature (b), and outlet moisture content (c, d) of obtained powders.

However, the model reflects the expected behavior of the spray dryer. Indeed, at the same temperature with different DE/GAE ratios, the simulated data show very similar trends to those obtained experimentally, where there is a higher final moisture content of particles when decreasing the amount of coating agent added to feed formulation. On the other hand, an expected behavior, predicted by the model, is that the final humidity of the particles has to decrease at higher inlet temperatures. However, the experimental outlet moisture contents of particles obtained at constant DE/GAE/ratio are not statistically different ($p > 0.01$). This could be explained by considering that the parameters related to the sorption isotherm and the relative drying rate were evaluated based on similar, but not equal, operating conditions. Thus, a difference between experimental and simulated data at constant temperature could be expected where, as mentioned, the model is capable to reflect the trend, but not the correct values. Secondly, the discrepancy might have been caused by the hygroscopic behavior of the encapsulated extract. Indeed, despite the precautions adopted during the experimental campaign, the encapsulated extract could have absorbed water vapor when put in contact with room humid air before being subjected to humidity measurements. This can explain why similar outlet moisture contents were measured at a constant DE/GAE ratio, even though the model does not foresee it. Despite this aspect must be studied in-deep for future applications, it is possible to verify what was previously affirmed. For this purpose, the potential absorption of water by the final particles is dependent on three main factors, namely their composition, outlet temperature, and the humidity of the air in the external environment. Therefore, assuming this last factor as negligible (i.e., considering constant air humidity in the room lab during the experimental campaign), it is possible to evaluate the fraction of water absorbed x_{water}^{plus} by powders, as reported in Eq. (16):

$$x_{water}^{plus} = (a x_{md}^{out} + b x_{ext}^{out})\,(T_p - T_{out}) \tag{16}$$

where x_{md}^{out} and x_{ext}^{out} are the outlet mass fraction of maltodextrins and natural extracts, respectively, while *a* and *b* are two constants. Therefore, the new moisture content of the particle, which considers also the hygroscopic effect, is calculated as follows (Eq. 17):

$$x_{water}^{new} = \frac{x_{water}^{plus} + x_{water}^{out,model}}{x_{water}^{plus} + x_{water}^{out,model} + x_{solid}^{out,model}} \quad (17)$$

Therefore, it is possible to affirm that hygroscopicity has affected the experimental results if, after evaluation of *a* and *b* parameters using non-linear regression routines in the BzzMath library, a good agreement between simulated and experimental data is obtained. The non-linear regression simulation calculated *a* and *b* equal to $1.1074 \cdot 10^{-4}$ and $1.7131 \cdot 10^{-3}$, respectively, thus leading to the results shown in the scatter diagram of Figure 1d. The results show an excellent agreement, confirming the hypothesis of a posterior water absorption after the spray-drying process. It is important to highlight that by regressing the parameters for hygroscopicity, the effects related to the estimation of the parameters of sorption isotherm or relative drying rate were masked. For this reason, as already mentioned, further experiments are needed in order to properly assess the two hypothesized effects. Additionally, the technical manual of the spray-dryer reports a residence time for the particles of about 1.0 seconds while their outlet dimensions have a size between 1 and 25 μm. Within this frame, Figure 2 reports the initial particle distribution and the final particle distribution predicted by the model, with the obtained values falling into the expected range, while the average residence time evaluated by the model was about 0.92 seconds.

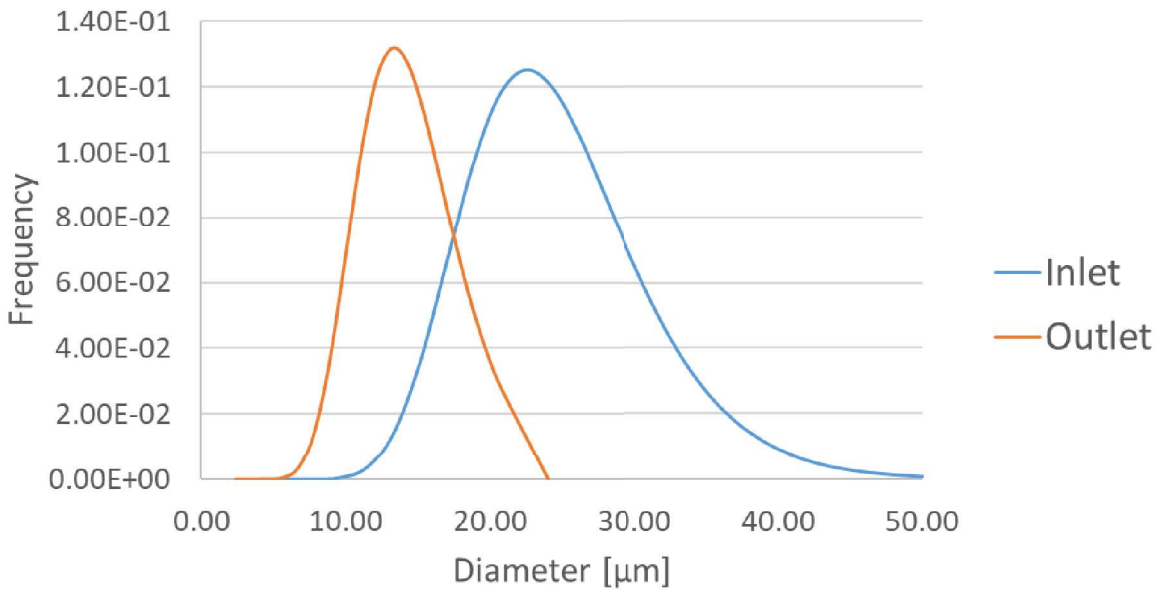

Figure 2. Particle size distribution curves of feed (inlet) and powder (outlet), as a function of the droplet or particle diameter.

Finally, the model can be used to evaluate different key parameters of the process like the change in outlet powder humidity along the spray dryer as shown in Figure 3. Interestingly, the lab spray-dryer reaches equilibrium conditions very early (≈ 0.1 m). Hence, the model could be used for future design optimization of the equipment.

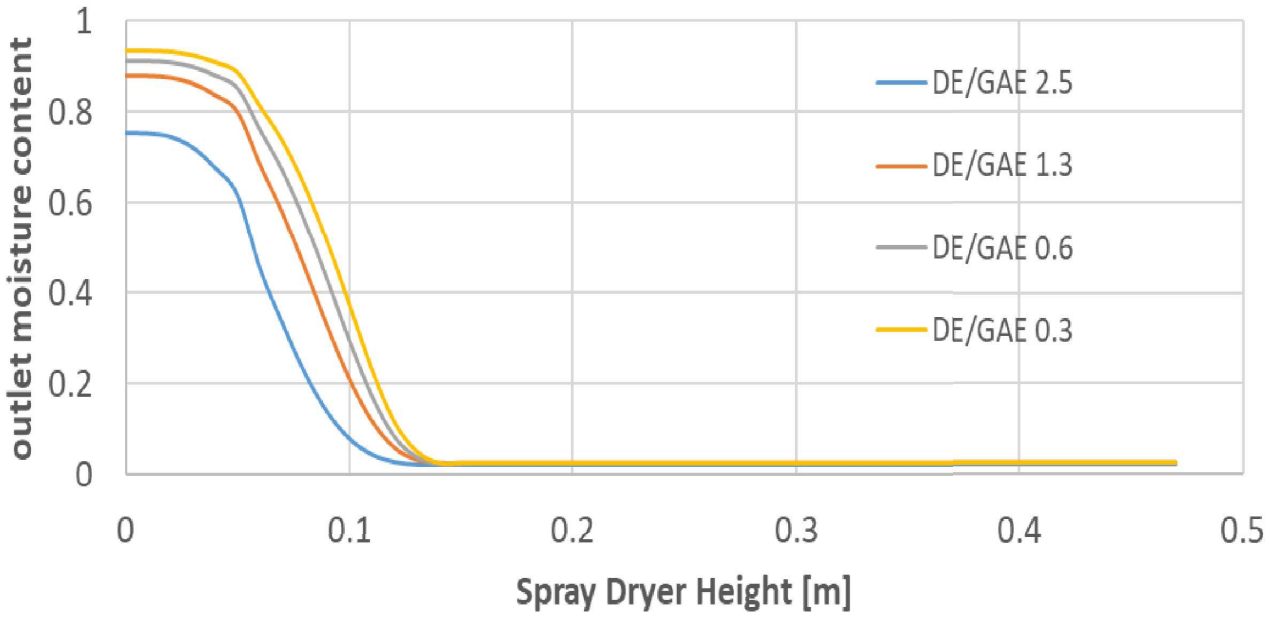

Figure 3. Evolution of droplet moisture content along the spray-drier as a function of the DE/GAE molar ratio. Air inlet temperature was set at 120°C.

Once the model has been validated, it was possible to use it for the evaluation of the kinetic parameters related to thermal degradation of polyphenols (Eq. 12). Similarly to model validation, proper experimental data were obtained, on which statistical analysis was performed, and then the data were used to regress the kinetic parameters. The experimental data obtained are shown in Table 2.

Table 2. Experimental (exp.) and simulated (sim.) values of total phenolic compounds concentration (c_{phe}) and their recovery obtained in the final powder, as a function of the different working inlet temperatures and DE/GAE molar ratios. Values were reported as means ± standard deviations.

T_{air_in} (°C)	DE/GAE	$c_{phe,in}$ (mg_{GAE}/g_{dw})	$c_{phe,out}$ (mg_{GAE}/g_{dw})		TPC recovery (%)	
		exp.	*exp.*	*sim.*	*exp.*	*sim.*
120	2.53	36.33	33.78 ± 5.20	33.77	92.99	92.97
120	1.12	69.61	56.60 ± 4.30	55.39	81.31	86.32
120	0.56	105.92	84.74 ± 2.82	81.48	80.00	81.73
120	0.28	143.29	117.67 ± 14.55	106.57	82.12	77.49
150	2.53	36.33	33.51 ± 0.76	33.78	92.23	92.95
150	1.12	61.18	55.73 ± 2.83	60.09	91.08	90.54
150	0.56	92.98	81.20 ± 2.33	86.57	87.33	87.62
150	0.28	125.64	110.77 ± 8.05	111.03	88.16	84.82

As expected, maltodextrins significantly influence the concentration of the bioactive compounds present in the recovered powders. Indeed, as already mentioned, maltodextrins protect bioactive compounds from thermal degradation, thus leading to a higher polyphenols recovery when increasing the DE/GAE ratio. The first step was to regress, using the BzzMath routines, the kinetic parameters A_0 and E_{ap} (Eq. 11), which have been calculated equal to $1.463 \cdot 10^{-6}$ (kg/s) and $3.043 \cdot 10^{2}$ (J/mol), respectively. The experimental and simulated data are also compared in the scatter diagram shown in Figure 4. The results show very good agreement, so it can be possible to describe the degradation of polyphenols through first-order kinetics.

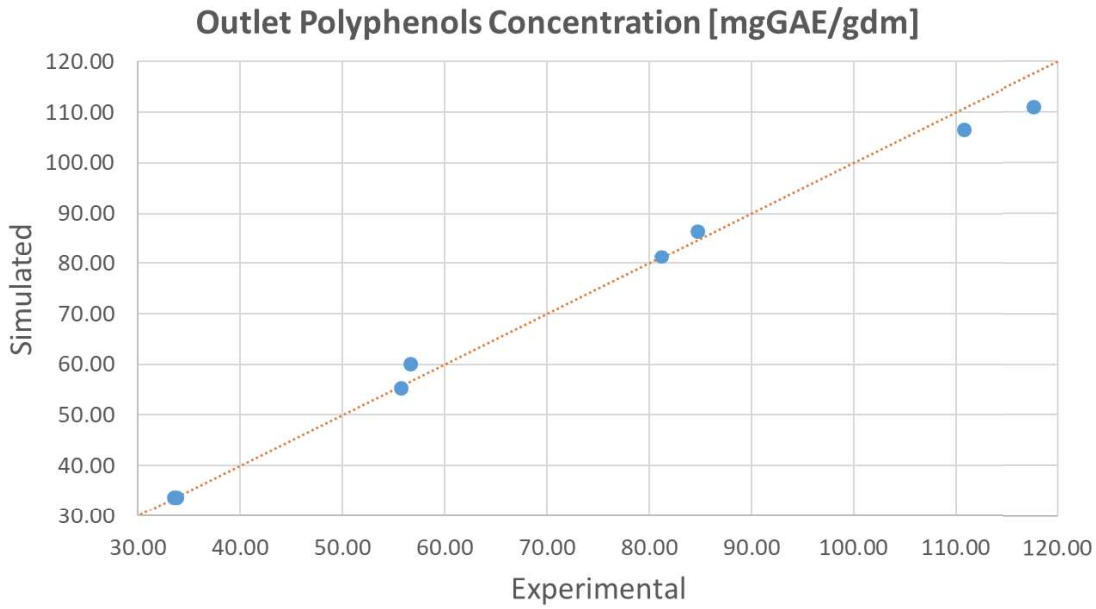

381

382 **Figure 4.** Scatter diagram of outlet polyphenols concentration in the obtained powders.

383 After adjusting the parameters, it is possible to evaluate the degradation of polyphenols along the
384 spray-drier (Figure 5). This aspect can be interesting for future optimization in terms of polyphenols
385 recovery. For instance, as shown, for a higher DE/GAE ratio, an equilibrium for polyphenols
386 degradation is reached and so a lower height of the spray-drier is enough to reach the same outlet
387 specifics. Conversely, for a lower DE/GAE ratio, this consideration could be not more possible.

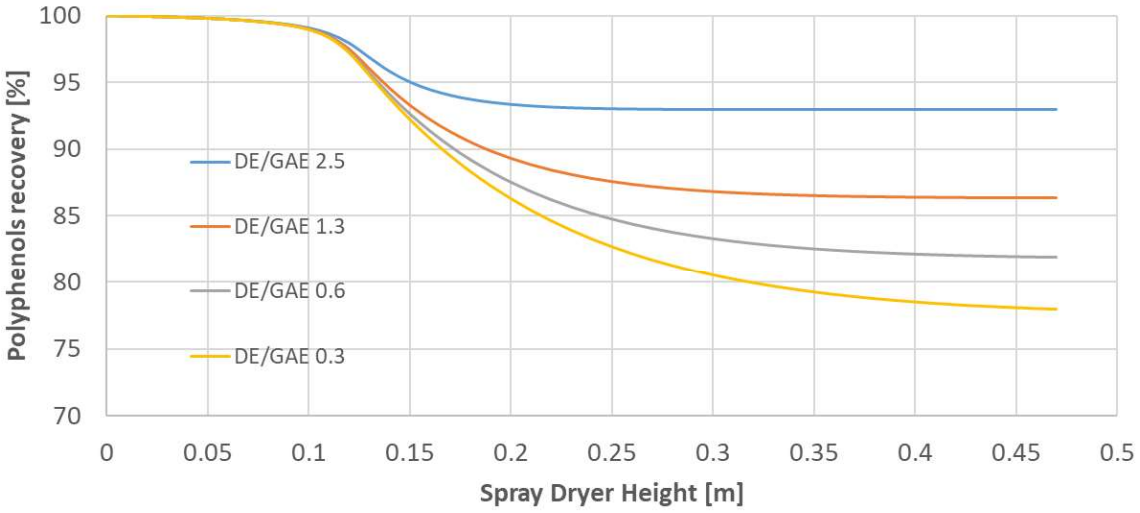

388

389 **Figure 5.** Evolution of polyphenols recovery along the spray-drier as a function of the DE/GAE molar
390 ratio. Air inlet temperature was set at 120°C.

The developed model could be applied also to a larger scale of the plant (i.e. pilot or industrial scale) and could be used in order to optimize the operating conditions or to estimate the loss on antioxidant activity of natural extracts at such scale. However, before making the simulation it is necessary to check the range applicability of the correlation used in this work. For instance, a parameter that has to be considered is the choice of atomizer and particle size, which could change the correlation in order to estimate the mean droplet size of a spray (Sormoli and Langrish, 2016). For sure, there are limitations in applying this model, such as the inability to predict potential hot or cold spots that may form inside the spray dryer that can further degrade the phenolic compounds thus reducing the quality of the encapsulated product. The prediction of hot and cold spots can be made through the use of computational fluid dynamics (CFD) models (Zbicinski et al., 2017). These models give in-deep information and are very useful for the design of the equipment, but, on the contrary, are not very suitable for optimization of operating conditions due to the high computational effort required. Regarding this, a future idea could be to couple the model developed in this study with a CFD simulation in order to obtain more useful information for a suitable process scale-up.

3.2. Modeling of spray-drying process for citrus fruit peels extracts

Finally, the model has been further validated through the simulation of the citrus extract encapsulation by means of cyclodextrins. Table 3 shows a good agreement between simulation and experimental data. The slight differences could be due to two different aspects. The main one is related to the different hygroscopicity between cyclodextrin and maltodextrins, as well as between citrus and Barbera extracts. The second aspect concerns the fact that the commercial citrus extract was solubilized in 0.5% NaOH solution (w/v) and probably the commercial citrus extracts have been already partially encapsulated by EVESA in order to increase their stability. As a final consideration,

415 it is possible to affirm that the outlet moisture content of samples does not appreciably vary for the
416 different kind of citrus extracts involved in the current study.

417

418 **Table 3.** Experimental (exp.) and simulated (sim.) values of outlet moisture content of encapsulated
419 different citrus extracts at constant cyclodextrins to citrus dry mass ratio (0.75) and constant inlet air
420 temperature (120°C). Values were reported as means ± standard deviations.

Citrus Extracts	Outlet Moisture (%)		
	exp.	*sim. (model)*	*sim. (model + hygroscopic effect)*
N 3-70	4.85 ± 0.30	2.65	6.91
N 10-60	4.61 ± 0.02	2.64	6.91
N 40-60	5.38 ± 0.02	2.65	6.92
N 28-20	5.21 ± 0.06	2.65	6.91

421

422 **4. Conclusions**

423 In this work, a mathematical model for the spray-drier assisted encapsulation of extracts deriving
424 from industrial food by-products was developed and subsequently validated, based on the
425 experimental trials performed as a function of the main processing parameters, namely the air inlet
426 temperature and the feed composition (e.g., molar ratio between natural extract and carrier agent).
427 Results demonstrated the potential of spray-drying technology to enable high recovery yields of
428 extracts (80 – 90 % w/w), and only slight thermal degradation of their antioxidant constituents,
429 described via first-order kinetics, was detected due to the protective effect exerted by the carrier agent.
430 Such outcomes were accurately predicted by the implied mathematical model, with significant
431 discrepancies observed only in the case of final particles moisture, which required the adoption of
432 further equations describing particles absorption of water vapor due to hygroscopic behavior.

In conclusion, further studies will involve the optimization of the whole spray-drying process, aiming to properly tune input parameters for the maximization of the recovery yields of solids, while preserving the integrity of target compounds via a reduced occurrence of temperature-mediated oxidation phenomena.

Acknowledgments

This research was financially European Union's Horizon 2020 Research and Innovation programme under grant agreement No 792261 (NewPack project).

References

1) Aliakbarian, B., Paini, M., Casazza, A.A., Perego, P. (2015). Effect of Encapsulating Agent on Physical-Chemical Characteristics of Olive Pomace Polyphenols-Rich Extracts. Chemical Engineering Transactions, 43, 97-102.
2) Amendola, D., De Faveri, D. M., Spigno, G. (2010). Grape marc phenolics: Extraction kinetics, quality and stability of extracts. *Journal of Food Engineering*, 97, 384-392.
3) Archaina, D., Leiva, G., Salvatori, D., Schebor, C. (2017). Physical and functional properties of spray-dried powders from blackcurrant juice and extracts obtained from the waste of juice processing. Food Science and Technology International, 24, 78–86.
4) Bassani, A., Montes, S., Jubete, E., Palenzuela, J., Sanjuan, A.P., Spigno, G. (2019). Incorporation of Waste Orange Peels Extracts into PLA Films. Chemical Engineering Transactions, 74, 1063-1068.
5) Bassani, A., Rossi, F., Fiorentini, C., Garrido, G. D., Reklaitis, G. V., Bonadies, I., & Spigno, G. (2020). Model of Spray-Drying for Encapsulation of Natural Extracts. Computer Aided Chemical Engineering, 48, 355-360.
6) Buzzi-Ferraris, G., & Manenti, F. (2010). Interpolation and regression models for the chemical engineer: Solving numerical problems. John Wiley & Sons.
7) Buzzi-Ferraris, G., & Manenti, F. (2015). Differential and differential-algebraic systems for the chemical engineer: solving numerical problems. John Wiley & Sons.
8) Chandrasekaran, M. (2013) Need for valorization of food processing by-products and wastes. In: Chandrasekaran, M. (Ed.), Valorization of Food Processing By-Products. Taylor & Francis Group, Florida, pp. 91–108.
9) Chasekioglou, A.N., Goula, A.M., Adamopoulos, K.G., Lazarides, H.N. (2017). An approach to turn olive mill wastewater into a valuable food by-product based on spray drying in dehumidified air using drying aids. Powder Technology, 311, 376–389.

10) Cotabarren, I.N., Bertín, D., Razuc, M., Ramírez-Rigo, M.V., Pina, J. (2018). Modelling of the spray drying process for particle design. Chemical Engineering Research and Design, 132, 1091–1104.

11) Dahiya, S., et al. (2018) Food waste biorefinery: Sustainable strategy for circular bioeconomy. *Bioresource Technology*, 248, 2 – 12.

12) Ding, Z., et al. (2020). Influences of different carbohydrates as wall material on powder characteristics, encapsulation efficiency, stability and degradation kinetics of microencapsulated lutein by spray drying. International Journal of Food Science and Technology, 55, 2872–2882.

13) Frontuto, D., Carullo, D., Harrison, S.M., Brunton, N.P., Ferrari, G., Lyng, J.G., Pataro, G. (2019). Optimization of Pulsed Electric Fields-Assisted Extraction of Polyphenols from Potato Peels Using Response Surface Methodology. Food Bioproc. Technol., 12, 1708-1720.

14) Galanakis, C.M. (2012). Recovery of high added-value components from food wastes: Conventional, emerging technologies and commercialized applications. Trends Food Sci. Technol., 26, 68–87.

15) Galanakis, C.M. (2015). Food Waste Recovery: Processing Technologies and Industrial Techniques. C.M. Galanakis Eds., ISBN: 978-0-12-800351-0.

16) Georgetti, S. R., Casagrande, R., Souza, C. R. F., Oliveira, W. P., Fonseca, M. J. V. (2008). Spray drying of the soybean extract: effects on chemical properties and antioxidant activity. LWT-Food Science and Technology, 41, 1521-1527.

17) Gharsallaoui, A., Roudaut, G., Chambin, O., Voilley, A., Saurel, R. (2007). Applications of spray-drying in microencapsulation of food ingredients: An overview. Food research international, 40, 1107-1121.

18) Green, D. W., Perry, R. H. (2008). Perry's Chemical Engineers' Handbook, 8th edition. New York: McGraw-Hill.

19) Goula, A. M., & Adamopoulos, K. G. (2005). Stability of lycopene during spray drying of tomato pulp. LWT- Food Science and Technology, 38, 479–487.

20) Goula, A. M., & Adamopoulos, K. G. (2006). Retention of ascorbic acid during drying of tomato halves and pulp. Drying Technology, 24, 57–64.

21) Goula, A.M., Lazarides, H.N. (2015). Integrated processes can turn industrial food waste into valuable food by-products and/or ingredients: The cases of olive mill and pomegranate wastes. Journal of Food Engineering, 167, 45–50.

22) Hanus, M. J., & Langrish, T. A. G. (2007). Re- entrainment of wall deposits from a laboratory-scale spray dryer. Asia- Pacific Journal of Chemical Engineering, 2(2), 90-107.

23) Jurmanovic, S., et al. (2019). Utilization of olive pomace as a source of polyphenols: Optimization of microwave-assisted extraction and characterization of spray-dried extract. Journal of Food and Nutrition Research, 58, 51-62.

24) Kaderides, K., Goula, A.M. (2019). Encapsulation of pomegranate peel extract with a new carrier material from orange juice by-products. Journal of Food Engineering, 253, 1–13.

25) Langrish, T.A.G. (2009). Degradation of Vitamin C in Spray Dryers and Temperature and Moisture Content Profiles in these Dryers. Food and Bioprocess Technology, 2, 400–408.

26) Lisboa, H.M., Duarte, M.E., Cavalcanti-Mata, M.E. (2018). Modeling of food drying processes in industrial spray dryers. Food and Bioproducts Processing, 107, 49–60.

27) Oliveira, B.E., et al. (2018). Spray-drying of grape skin-whey protein concentrate mixture. J Food Sci Technol, 55, 3693–3702.

28) Osorio-Arias, J., et al. (2020). New powder material obtained from spent coffee ground and whey protein; Thermal and morphological analysis. Materials Chemistry and Physics, 240, 122171.

29) Marques, H. M. C. (2010). A review on cyclodextrin encapsulation of essential oils and volatiles. Flavour and fragrance journal, 25(5), 313-326.

30) Pataro G., Carullo D., Bobinaite R., Donsi G., Ferrari G. (2017). Improving the extraction yield of juice and bioactive compounds from sweet cherries and their by-products by pulsed electric fields. *Chemical Engineering Transactions*, 57, 1717-1722.

517 31) Permal, R., Chang, W.L., Seale, B., Hamid, N., Kam, R. (2020a). Converting industrial organic
518 waste from the cold-pressed avocado oil production line into a potential food preservative. Food
519 Chemistry, 306, 125635.
520 32) Permal, R., Chang, W.L., Chen, T., Seale, B., Hamid, N., Kam, R. (2020b). Optimising the Spray
521 Drying of Avocado Wastewater and Use of the Powder as a Food Preservative for Preventing
522 Lipid Peroxidation. Foods, 9, 1187.
523 33) Sepelevs, I., Zagorska, J., Galoburda, R. (2020). A food-grade antioxidant production using
524 industrial potato peel by-products. Agronomy Research, 18, 554–566.
525 34) Schmitz-Schug, I., Kulozik, U., Foerst, P. (2016). Modeling spray drying of dairy products –
526 Impact of drying kinetics, reaction kinetics and spray drying conditions on lysine loss. Chemical
527 Engineering Science,141, 315–329.
528 35) Sormoli, M.E., Langrish, T.A.G. (2016). The use of a plug-flow model for scaling-up of spray
529 drying bioactive orange peel extracts. Innovative Food Science and Emerging Technologies, 37,
530 27–36.
531 36) Spigno, G., Tramelli, L., De Faveri, D. M. (2007). Effects of extraction time, temperature and
532 solvent on concentration and antioxidant activity of grape marc phenolics, Journal of food
533 engineering, 81, 200-208.
534 37) Spigno G., Amendola D., Dahmoune F., Jauregi P. (2014). Colloidal gas aphrons based separation
535 process for the purification and fractionation of natural phenolic extracts. Food and Bioprod.
536 Process., 94, 434-442.
537 38) Toledo-Madrid, K.I., Gallardo-Velázquez, T.G., Terrazas-Valencia, F., Osorio-Revilla, G.I.
538 (2019). Spray drying microencapsulation of purple cactus pear (Opuntia ficus indica) peel extract
539 and storage stability of bioactive compounds. Emirates Journal of Food and Agriculture,31, 958-
540 968.

541 39) Truong, V., Bhandari, B. R., Howes, T. (2005). Optimization of co-current spray drying process
542 of sugar-rich foods. Part I - Moisture and glass transition temperature profile during drying.
543 *Journal of Food Engineering*, 71, 55-65.
544 40) Utpott, M., et al. (2020). Evaluation of the Use of Industrial Wastes on the Encapsulation of
545 Betalains Extracted from Red Pitaya Pulp (Hylocereus polyrhizus) by Spray Drying: Powder
546 Stability and Application. Food and Bioprocess Technology, 13, 1940–1953.
547 41) Velazquez-Martinez, V., Valles-Rosales, D., Rodriguez-Uribe, L., Holguin, O., Quintero-Quiroz,
548 J., Reyes-Jaquez, D., Delgado, E. (2021). Antimicrobial, Shelf-Life Stability, and Effect of
549 Maltodextrin and Gum Arabic on the Encapsulation Efficiency of Sugarcane Bagasse Bioactive
550 Compounds. *Foods*, *10*(1), 116.
551 42) Wang, S., Langrish, T.A.G. (2009). A distributed parameter model for particles in the spray
552 drying process. Advanced Powder Technology, 20, 220–226.
553 43) Waterhouse, G.I.N., Waterhouse, D.S., Su, G., Zhao, H., Zhao, M. (2017). Spray-Drying of
554 Antioxidant-Rich Blueberry Waste Extracts; Interplay Between Waste Pretreatments and Spray-
555 Drying Process. Food Bioprocess Technol, 10, 1074–1092.
556 44) Zhang, R., et al. (2020). Microencapsulation of anthocyanins extracted from grape skin by
557 emulsification/internal gelation followed by spray/freeze-drying techniques: Characterization,
558 stability and bioaccessibility. LWT - Food Science and Technology, 123, 109097.
559 45) Zanoni, F., Primiterra, M., Angeli, N., Zoccatelli, G. (2020). Microencapsulation by spray-drying
560 of polyphenols extracted from red chicory and red cabbage: Effects on stability and color
561 properties. Food Chemistry, 307, 125535.
562 46) Zbicinski, I. (2017). Modeling and Scaling Up of Industrial Spray Dryers: A Review. Journal of
563 Chemical Engineering of Japan, 50, 757-767.